
Assessing food limitation for marine juvenile fishes in coastal nurseries using a bioenergetic approach

Lefebvre Du Prey Marion ^{1,*}, Lobry Jérémy ¹, Brind'Amour Anik ², Le Bris Hervé ³, Sadoul Bastien ³

¹ INRAE, UR EABX, Cestas Cedex, France

² DECOD (Ecosystem Dynamics and Sustainability: from source to sea), Ifremer, Institut Agro, INRAE, Nantes, France

³ DECOD (Ecosystem Dynamics and Sustainability: from source to sea), Institut Agro, INRAE, Ifremer, Rennes, France

* Corresponding author : Marion Lefebvre Du Prey, email address : marion.lefebvre-du-prey@inrae.fr

Abstract :

Understanding mechanisms affecting the renewal of populations is critical for species' conservation and living resources management. For fish species, density-dependant mechanisms occurring in young stages are particularly well studied. The food limitation hypothesis assumes that the food availability is the main limiting factor for juveniles' growth and survival in coastal and estuarine nurseries. Although some promising modelling methods appeared to test this hypothesis, it remains debated because of a lack of a clear signal of food limitation. We use a mechanistic approach based on DEB (Dynamic Energy Budget) theory to test the trophic limitation hypothesis from a metabolic point of view. The energy intake of individuals is quantified given the experienced temperatures, and measures of individuals' length-at-age. We reconstruct the food ingested in an "inverse"-DEB modelling. Then, we further explore the potential of inverse-DEB modelling to describe in fine details the energy partitioning between the main metabolic processes (i.e., maintenance, maturation and growth) of an individual, and highlight periods of energy shortage indicating a trophic limitation. As a case study, we implemented this approach for the juveniles of common sole (*Solea solea*) settled between 2000 and 2014 in the Seine estuarine nursery. Our approach allowed to (i) quantify food assimilation, and identify (ii) a decrease in the growth efficiency, and (iii) the occurrence of nutritional stress. Both the decrease in growth and the periods of nutritional stress coincide with a decrease in individual-specific food availability. Therefore, the inverse-DEB approach is an interesting tool to test the food limitation hypothesis at the individual scale. DEB theory deepens and structures our knowledge on energy intake and energy use, hence suggesting concrete indices of trophic limitation such as periods of non-growing, and nutritional stress due to starvation (i.e. no food intake). Work on the parametrization of the DEB model is progressing rapidly and our method can already be generalized to other fish species. Finally, mechanistic description of food limitation using bioenergetic modelling helps better understanding the ecology of the species in a dynamic environment. This may ultimately help going towards better species' conservation and fisheries management.

Highlights

► Trophic limitation hypothesis is tested for juvenile soles in a coastal nursery. ► Inverse-DEB modelling estimates food ingested from temperatures and fish's lengths. ► Food assimilation and energy partitioning over time are investigated. ► Periods of non-growing and nutritional stress indicate a trophic limitation. ► Food limitation at the individual scale occurs in late summer.

Keywords : DEB model, Energy partitioning, Estuaries, Flatfishes, Nutritional stress

1. INTRODUCTION

1.1 The food limitation hypothesis in coastal and estuarine nurseries

Understanding mechanisms affecting the renewal of populations is critical for species' conservation and living resources management. For fish species, we know that regulation factors occurring at larval and juvenile stages directly affect their recruitment (*i.e.* when the young fishes reach the adult stock), mainly through size-selective maturation and size selective survival (Daewel et al., 2011; Van Der Veer et al., 1994). The trophic limitation hypothesis assumes that the environment can supply only finite food resources, restraining the number of individuals able to correctly develop, grow and survive (Amara et al., 2000; Nash et al., 2007; Nunn et al., 2012). Trophic limitation might cause nutritional stress (Neill et al., 1994), resulting in reduced growth and body condition (Meyer et al., 2012), and ultimately in death.

Many young fish, including juvenile flatfishes concentrate in coastal and estuarine (C&E) shallow waters to grow and mature before their recruitment. Indeed, C&E areas offer particular conditions (*e.g.*, high food supply, protection against predation) that allow them to act as nursery grounds for marine juvenile flatfishes, often of fisheries interest (Le Pape et al., 2003; Seitz et al., 2014). However, global changes affecting C&E areas (*e.g.* coastline modification or pollution) may have led, in numerous cases, to a decline in their nursery function (Rochette et al., 2010; van der Veer et al., 2022). During the last decade, particular attention was drawn towards the hypothesis of trophic limitation for juvenile flatfishes in C&E nurseries (Le Pape & Bonhommeau, 2015), with growth reduction observed for juveniles in several areas across the North-West Atlantic (Cardoso et al., 2016; Freitas et al., 2012; Poiesz et al., 2020; van der Veer et al., 2010).

1.2 Existing methods to identify a trophic limitation

Several approaches were proposed to test the trophic limitation hypothesis for juvenile fishes in C&E nurseries, leading to contrasting conclusions according to the review of Le Pape and

26 Bonhommeau (2015). When exploring this hypothesis at the individual scale, most rejected it (*e.g.*
27 Gilliers et al., 2006; Selleslagh & Amara, 2013). However, variations in juvenile's condition were
28 observed (*e.g.* for the plaice, Ciotti et al., 2014), and are likely related to starvation. Le Pape and
29 Bonhommeau (2015) explain that, in fact, size-selective mortality and size-selective sampling might
30 hide the effect of food limitation: (1) small individuals in poor condition are more likely to be dead
31 at the time of sampling and (2) they are likely less captured by the classic fishing gears. On the other
32 hand, when focusing at the population scale, studies mainly support the trophic limitation
33 hypothesis. Indirect population scaled approaches revealed indicators of food limitation such as (i)
34 food partitioning (*e.g.* Amara et al., 2001), (ii) link between fishes' distribution and energy
35 availability at the individual scale (*e.g.* Nicolas et al., 2007), or (iii) growth and condition reduction
36 in comparison to optimal environments (Freitas et al., 2012; van der Veer et al., 2010).

37 Therefore, trophic limitation hypothesis is still discussed because of the lack of an obvious
38 signal of food limitation occurring on surviving juveniles (Le Pape & Bonhommeau, 2015). During
39 the last years, several authors used a direct population scaled approach to test the trophic limitation
40 in C&E nurseries at the juvenile fish community level, based on the calculation of the exploitation
41 efficiency (EE) (Day et al., 2021; Saulnier et al., 2020; Tableau et al., 2019). This method consists
42 in the assessment of a predation pressure, through the calculation of a ratio between the food
43 consumed by predators and the food supplied by prey (Collie, 1987; Vinagre & Cabral, 2008). Food,
44 and thus energy consumed can be approached by a simple model as proposed by Tableau et al.
45 (2019). The recent studies using this method support the trophic limitation hypothesis for juvenile
46 flatfishes in the Seine estuarine nursery, mainly at the end of the growth period (*i.e.*, late summer
47 and autumn) (Day et al., 2021; Saulnier et al., 2020).

48 These latter approaches seem relevant and promising toward community level as they
49 combine data at population and individual levels. However, they also come with multiple
50 constraints. First, population scale growth rates, distribution or energy consumption datasets are
51 rarely available because of the time-consuming field and laboratory works they require (Saulnier et
52 al., 2020). Regarding the EE model of Tableau et al. (2019), it also requires a lot of work because

53 of the need to consider the whole community of prey and predators (Tableau et al., 2016).
54 Additionally, energy consumption in this model is assumed proportional to growth, ignoring energy
55 requirements when growth is null. Finally, the growth efficiency coefficient used to convert
56 observed growth into energy consumption is constant in this model, irrespective of environment
57 variations such as temperature. Yet, energy consumption might be very variable, depending on the
58 environment, the season, the size of the individual and the energy required for its maintenance
59 (Kooijman, 2010).

60 Therefore, although modelling approaches largely improve our knowledge on prey
61 availability for juvenile flatfishes in nursery grounds (Tableau et al., 2019), testing the trophic
62 limitation hypothesis requires new tools to assess individuals food intake and physiological
63 condition in a dynamic environment (Ciotti et al., 2014).

64 **1.3 The DEB modelling to test the trophic limitation hypothesis**

65 Dynamic Energy Budget (DEB) theory is an integrative theory of energy allocation that
66 describes and quantifies the metabolism of an individual over its whole lifecycle, in varying
67 environmental conditions, *i.e.* temperature and food availability (Kooijman, 2000; Marques et al.,
68 2018; Nisbet et al., 2000; Van der Meer, 2006). A powerful aspect of models based on DEB theory
69 (DEB models) is also the possibility to back-calculate energy ingestion, based on experienced
70 temperatures and observed growth patterns (Cardoso et al., 2006; Freitas et al., 2009, 2011;
71 Kooijman, 2010; Pecquerie et al., 2012). This inverse-DEB modelling has been used to reconstruct
72 time series of food availability and energy consumption for several bivalves species (e.g. Cardoso
73 et al., 2006; Freitas et al., 2009; Lavaud et al., 2019). Also, Pecquerie et al. (2012) used this method
74 in order to study the capacity of otoliths data to provide more detailed information on the growth
75 history of the individual, and on the energy it assimilated in the field. These studies showed that
76 reconstructing energy ingestion using inverse-DEB modelling constitutes an original and relevant
77 framework to learn more about fluctuations of resources available for the studied species, as well as
78 of their energy intake and use.

79 DEB modelling might address the difficulties previously referred in the assessment of the
80 trophic limitation in C&E nurseries. DEB model considers that individuals consume energy even
81 when they don't grow, for their maintenance and maturation (Kooijman, 2010). Thus it allows a
82 more accurate information on fishes' energy intake through time than the EE model of Tableau et
83 al. (2019) that considers a constant linear link between observed growth and energy consumption.
84 Therefore, inverse-DEB modelling might constitute a relevant tool to test the trophic limitation
85 hypothesis for juvenile fishes in C&E nurseries. Freitas et al. (2011) used this approach to test
86 trophic limitation hypothesis for the sand goby over the period of nursery residence. Their approach
87 consisted in reconstructing the mean scaled food conditions over the lifetime of individuals, by
88 comparing the observed asymptotic length with the theoretical maximum one (under unlimited food
89 conditions).

90 We propose here to (i) apply the inverse-DEB modelling approach to a large dataset of
91 growth trajectories of *Solea solea*, and (ii) go further in exploring the potential of DEB models to
92 detect nutritional stress periods in fish based on fine description of their energy partitioning. We
93 focus on the juveniles of the common sole (*Solea solea*) in the Seine estuarine nursery. We first use
94 inverse-DEB modelling to reconstruct the dynamic of individual-specific food conditions in the
95 nursery. Then, we study the energy partitioning, that is the distribution of mobilized energy between
96 the different metabolic processes considered by the DEB model (*i.e.*, maintenance, growth and
97 maturation), under the experienced environmental conditions. This method allows us to identify
98 indices of trophic limitation such as growth reduction and periods of nutritional stress.

99 **2. MATERIAL AND METHODS**

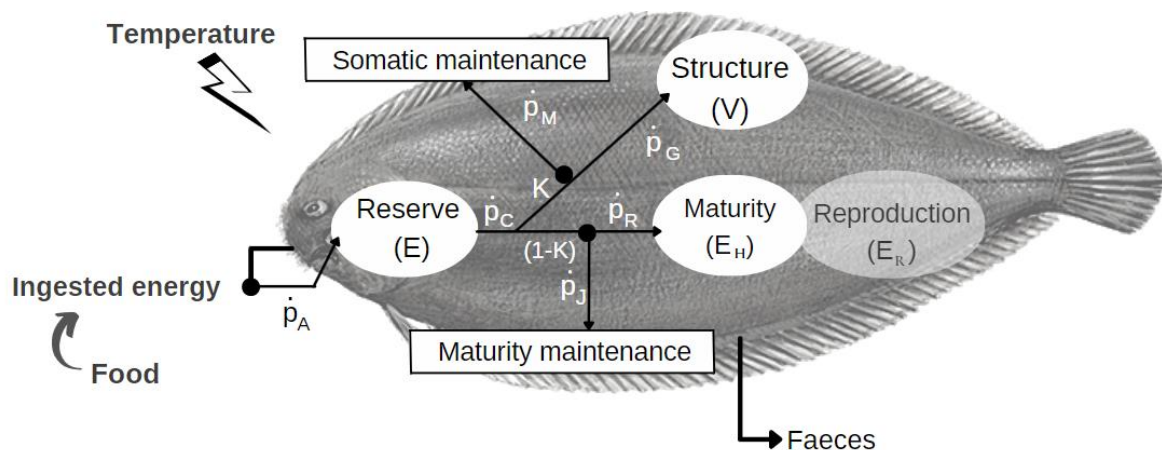
100 **2.1 DEB theory**

101 **2.1.1 State variables and fluxes**

102 DEB theory describes and quantifies the metabolism of an individual through four state variables
103 that are linked to mass and metabolic processes (see Figure 1) (Kooijman, 2010; Marques *et al.*, 2018;

104 Van der Meer, 2006). The reserve E (J) translates the available energy for metabolic processes such as
 105 growth, maintenance, development and reproduction in adults. The structure V (cm^3) corresponds to the
 106 organism's somatic parts. The maturity compartment E_H quantifies the cumulated energy invested into
 107 development (maturation). Finally, the reproduction compartment E_R (J), filled once the puberty starts,
 108 allows the production of offspring (here E_R is fixed to zero as the study only concerns juveniles). The
 109 state variables are supplied in energy at rates ($\text{J} \cdot \text{d}^{-1}$) that depend on environmental conditions (*i.e.*,
 110 temperature and food) and on the state of the organism (Kooijman, 2010; Sousa *et al.*, 2010; Van der
 111 Meer, 2006). Before its birth, the individual uses energy stocked into its reserve but does not assimilate
 112 energy. From the moment it is born (*i.e.* for fish the beginning of the exotrophic phase of the larvae),
 113 the organism feeds and starts assimilating energy from its environment at a rate \dot{p}_A . This assimilated
 114 energy fills the reserve compartment E , from which it will be mobilized at a rate \dot{p}_C . From the flow of
 115 mobilized energy, a fraction $\kappa\dot{p}_C$ will be allocated to the growth of structure and the somatic
 116 maintenance. A primary flow \dot{p}_M goes to the somatic maintenance while the remaining energy will go
 117 into growth (\dot{p}_G). The rest of the mobilized energy, $(1-\kappa)\dot{p}_C$, will be allocated in priority to the
 118 maintenance of maturity (\dot{p}_J), and then to the maturity (\dot{p}_R). State variables and fluxes considered in
 119 the DEB model are described in Table 1 and Figure 1.

120



121

122 Figure 1: Conceptual representation of the Dynamic Energy Budget (DEB) model. The circles are the

123 state variables: Reserve E (J), structure V (cm^3), maturity E_H (J) and reproduction buffer E_R (J). The124 arrows represent the energy fluxes ($\text{J} \cdot \text{d}^{-1}$). The rectangles are the maintenance compartments. The

125 temperature and food are the two environmental variables considered in the DEB model.

126 Table 1: Names, equations and units of state variables and metabolic processes in DEB theory for an
 127 individual at the juvenile stage (Kooijman, 2010).

State variable	Differential equation	Unit
Reserve	$\frac{dE}{dt} = \dot{p}_A - \dot{p}_C$	J
Structure	$\begin{array}{ l} \text{if } \kappa \dot{p}_C \geq \dot{p}_M : \\ \frac{dV}{dt} = \frac{\dot{p}_G}{[E_G]} \end{array} \quad \left \quad \begin{array}{l} \text{if } \kappa \dot{p}_C \leq \dot{p}_M : \\ \frac{dV}{dt} = \frac{\dot{p}_G}{\kappa_G [E_G]} \end{array}$	cm ³
Maturity	$\frac{dE_H}{dt} = \dot{p}_R$	J
Reproduction buffer	$\frac{dE_R}{dt} = 0$	J
Metabolic processes	Equation	Unit
Assimilation	$\dot{p}_A = \{\dot{p}_{Am}\} f L^2$	J/d
Mobilization	$\dot{p}_C = \frac{[E_G] \dot{v} V^{-1/3} + [\dot{p}_M]}{\frac{[E_G]}{E} + \frac{\kappa}{V}}$	J/d
Somatic maintenance	$\dot{p}_M = [\dot{p}_M] V$	J/d
Growth	$\dot{p}_G = \kappa \dot{p}_C - \dot{p}_M$	J/d
Maturity maintenance	$\dot{p}_J = \dot{k}_j E_H$	J/d
Maturation	$\dot{p}_R = (1 - \kappa) \dot{p}_C - \dot{p}_J$	J/d

128

129

2.1.2 Consideration of the environment

130 In order to account for the effect of temperature on metabolic rates, the parameters $\{\dot{p}_{Am}\}$, \dot{v} ,

131 $[\dot{p}_M]$ and \dot{k}_j are corrected by a temperature correction factor TC (Kooijman, 2010) (see Appendix A

132 for further information). In the calculation of \dot{p}_A (see Table 1), the variable f is the scaled functional
 133 response (Kooijman, 2010), and links the food density in the environment with the actual amount
 134 of energy ingested by the animal. f allows the energy assimilation rate of the individual to be scaled
 135 in relation to the maximum one $\{\dot{p}_{Am}\}$. Therefore, it is usually considered between 0 and 1, with
 136 $f=0$ corresponding to a state of starvation (*i.e.* no food intake) and $f=1$ implying an assimilation rate
 137 that is equal to the theoretical maximum specific assimilation rate, $\{\dot{p}_{Am}\}$. According to Freitas et
 138 al., 2011, f can be used as a proxy of the available food in the environment. However, the term
 139 “individual-specific” here highlights that it translates apparent scaled food conditions for an
 140 individual and not to the whole amount of food available in the environment. This is important, as f
 141 is the integration of multiple factor including energy available in the environment, but also intra and
 142 inter-specific competition. In other words, it is related to the energy that can actually be ingested
 143 and then assimilated by an individual.

144 **2.1.3 Calculating length over time**

145 Given daily temperatures, food availability and the species-specific parameters of the model (see
 146 Appendix A), DEB theory can predict the individual structural length L , which corresponds to $V^{1/3}$.

147 When nutritional stress occurs, energy mobilised is no longer sufficient to cover the somatic
 148 maintenance requirements, (*i.e.* $\kappa\dot{p}_C < p_M$). In this case, we consider that shrinking of structure is
 149 allowed to fulfil these somatic maintenance requirements (implying that \dot{p}_G can be negative). The
 150 mobilized energy is assumed to be equal to $\frac{1}{\kappa_G} \frac{dV}{dt}$ (see Table 1), with κ_G the growth efficiency,
 151 calculated as : $\kappa_G = d_v q_v / [E_G]$ (Mounier, 2019), where d_v , q_v and $[E_G]$ are the density, energy density,
 152 and cost per unit of structure (see Appendix A).

153 The physical length L_w (*cm*) is calculated from the structural length and a shape coefficient δ ,
 154 assuming isomorphy and no contribution of reserve to physical length: $L_w = L/\delta$. Shape coefficient δ is
 155 unitless, and constant post-metamorphosis according to Mounier et al.(2020). It is important to note that
 156 a different structure to physical length relationship should be considered when shrinking happens,
 157 however we decided to keep δ constant whether the individual is under nutritional stress or not, as in

158 Augustine et al. (2011). This allows simplifying our method, and we consider that the results will not
 159 change significantly.

160 **2.2 Implementing an inverse-DEB modelling to reconstruct food ingestion**

161 All the modelling steps of this study (*i.e.* paragraphs 2.2 and 2.3) were implemented in R (R Core
 162 Team 2021) and the integrated development environment (IDE) R-studio (Rstudio Team 2020).

163 As a first step, we back-calculated the scaled functional response (f) to assess the food ingested by
 164 individuals, given the experienced temperatures and observed individuals length-at-age. Age of the fish
 165 is estimated in days post fertilization (dpf), assuming a unique fertilization date. To better represent the
 166 temporal variability of food ingestion, one f value was calculated for each period between two length
 167 observations, and independently for individuals of each age class (*i.e.*, each cohort - a cohort represents
 168 the individuals born in the same year). Thus, for each period, we estimated f by minimising the Mean
 169 Relative Error (MRE) between the observed lengths (L) and the lengths estimated using the DEB model
 170 (\hat{L}) for each time point (i) with an observation of the period (1).

$$171 \quad MRE = \frac{1}{n} \sum_{i=m}^{m+n} \left(\frac{|L_i - \hat{L}_i|}{L_i} \right) \times 100$$

172 (1)

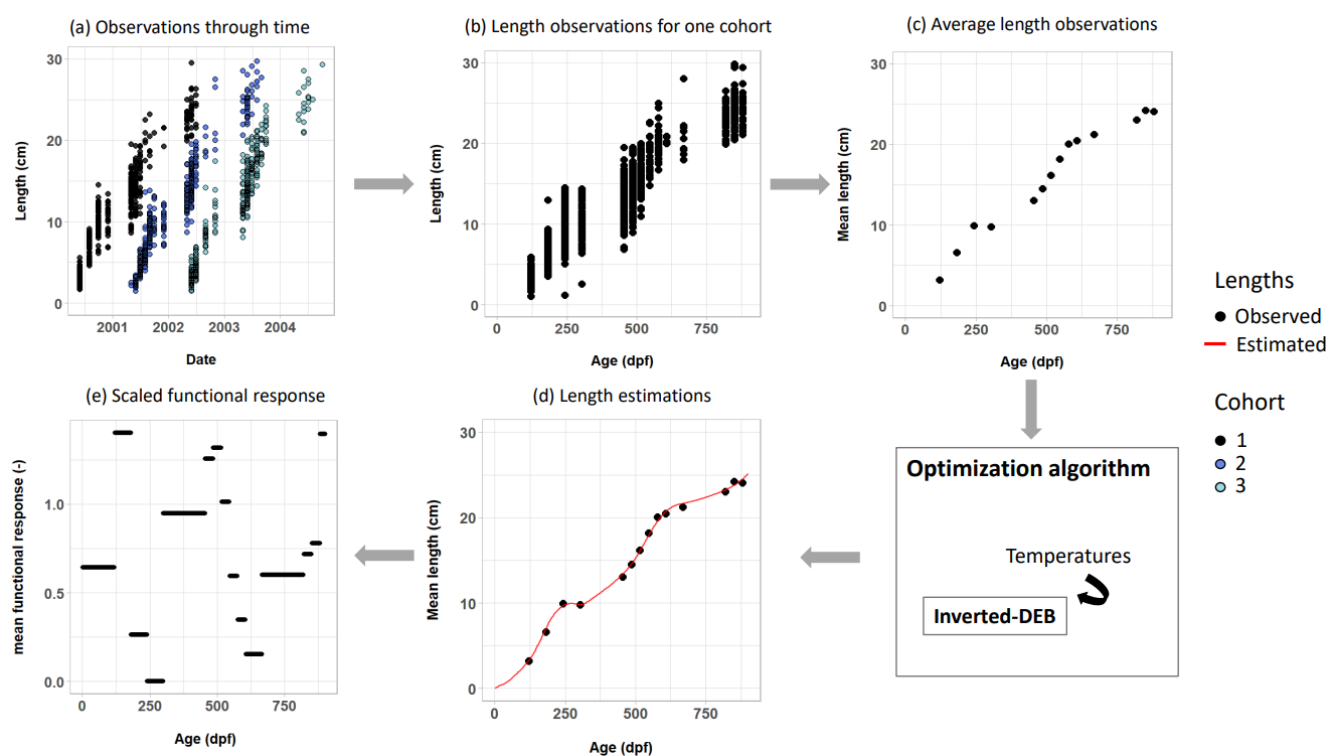
173 The “optim” function (R Core Team 2021) with the method “L-BFGS-B ” (Byrd et al., 1995)
 174 was used.

175 To simplify this optimization step, the observed lengths were averaged within each cohort and
 176 time point, so that an average individual from each cohort is represented through the three years within
 177 the nursery. Figure 2 resumes our methodology for the back-calculation of individual-specific food
 178 conditions.

179 During the step of parametrization of the DEB model, the maximum assimilation rate $\{p_{Am}\}$ is
 180 determined by experiments or found in the literature. In the present study, during the optimization
 181 process, we allowed f to take values greater than 1. While it is not classical in DEB studies, f values can

182 be greater than 1 as long as f is not considered as an explicit functional response for a given food
 183 concentration but only as a proxy for the food. In that context, this implies that f embeds the uncertainty
 184 in both \dot{p}_X and $\{\dot{p}_{Am}\}$ considering that (i) the food quality in the nursery could be better than those used
 185 for calibrating the DEB model, and (ii) there is a possible genetic variability in $\{\dot{p}_{Am}\}$ between
 186 populations. A f greater than 1 implies an assimilation rate superior to $\{\dot{p}_{Am}\}$. This idea is supported by
 187 some observations *in natura* of growth rates higher than those simulated by the DEB model for a $f=1$
 188 (e.g. for the bivalve *Macoma balthica*, in Cardoso *et al.* (2006)). We therefore allow f to take values
 189 above 1 and limited it to a maximum of 2. This choice is supported by preliminary calculations of values
 190 of f that (i) are theoretically allowable and (ii) are already used for predictions, showing satisfying fit of
 191 the model to the data for *S. solea* (AmP Solea solea, version 2021/11/30). The final distribution of f
 192 values is visible in Appendix D. In order to facilitate the interpolation of f between two observations (to
 193 get a daily value of f), we assumed f constant during the period between two samplings (see Figure 2).

194



195

196 Figure 2: Conceptual representation of the methodology for the reconstruction of individual-specific
 197 food conditions (*i.e.* scaled functional response). Length data are available over time (a). From the

198 lengths of the individuals of one cohort over age in dpf (b), the average lengths were calculated and
199 used in the inverse-DEB modelling (c). By minimizing the MRE between these lengths and the ones
200 estimated by the DEB model (d), we back-calculated the scaled functional response (e). See section
201 2.2 for further explanations on the values of the scaled functional response in the figure.

202 **2.3 Simulate metabolism under experienced conditions**

203 **2.3.1 Energy intake over time**

204 We simulated the metabolism of an average individual every day for the three years spent in the
205 nursery, under experienced temperatures.

206 For *Solea solea*, $\{\dot{p}_{Am}\}$ is different between males and females (see Appendix A), and therefore
207 daily assimilated energy in a same environment varies between sexes. However, hereafter we adjusted
208 a value of f from the same observed lengths independently for a male and a female. Then we averaged
209 all the simulations to present the results for an average individual, on the assumption that the
210 observations are half from females and half from males.

211 The daily-assimilated energy \dot{p}_A (see Table 1) actually corresponds to the daily-consumed
212 energy \dot{P}_X divided by a digestibility coefficient κ_X (fixed to generalized animal value (Mounier et al.,
213 2020) – see Appendix A). Therefore, the daily-consumed energy was calculated for an average
214 individual as $\dot{p}_X = \dot{p}_A/\kappa_X$.

215 **2.3.2 Energy partitioning**

216 Once the energy intake was calculated, we studied the energy partitioning, particularly in order
217 to assess individuals' growth capacity, and to identify potential periods of nutritional stress. To do so,
218 the absolute fluxes towards growth, maturation, maturity maintenance and somatic maintenance were
219 calculated (in *kJ/day*), as well as the percentage of mobilized energy allocated to each metabolic process,
220 respectively.

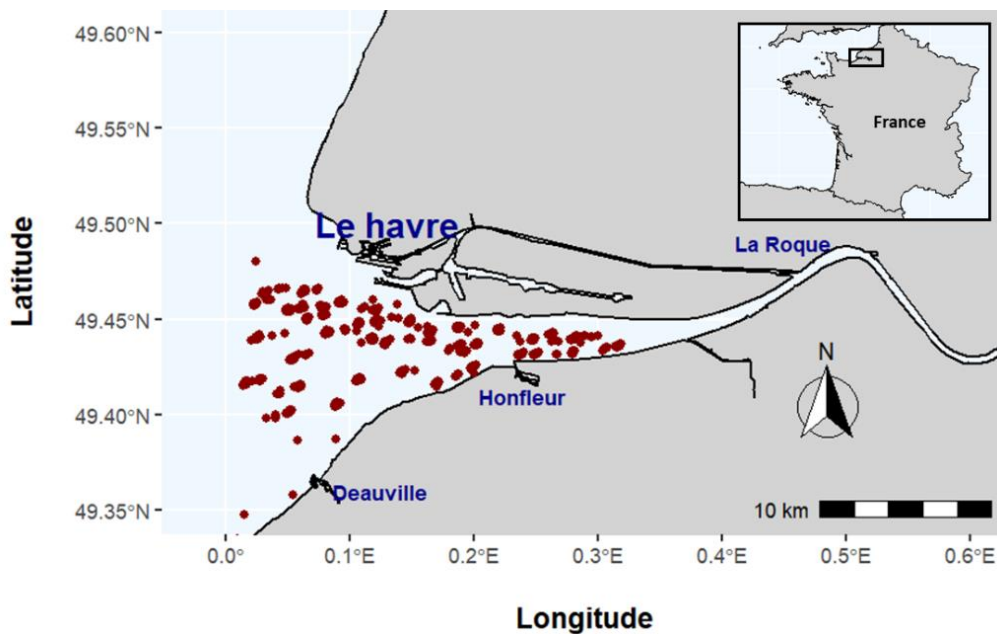
221 **2.3.3 Growth efficiency**

222 The variable that links growth with energy consumption is the growth efficiency coefficient (k),
223 *i.e.*, the quantity of energy required by the organism to allocate one energy unit into the structure. The
224 growth efficiency within DEB theory is generally calculated as the ratio between the amount of energy
225 fixed into structure and the amount of ingested energy (\dot{p}_A/κ_X , or \dot{p}_X). However, \dot{p}_C is used here instead
226 of \dot{p}_A in order to avoid calculation issues due to possible null values of \dot{p}_A . Therefore, the growth
227 efficiency coefficient k is calculated as: $k = (\dot{p}_G\kappa_G)/(\dot{p}_C/\kappa_X)$. \dot{p}_G is the quantity of energy daily
228 allocated to growth, corrected by κ_G (*i.e.* growth efficiency), in order to consider the energy that is
229 actually fixed into structure. \dot{p}_C is the daily quantity of mobilized energy, and is divided by κ_X
230 (digestibility coefficient, see Appendix A), in order to approximate the daily quantity of consumed
231 energy.

232 **2.4 Case study: the common sole in the Seine estuarine nursery**

233 **2.4.1 Study site**

234 To illustrate our proposal, we used the case study of the juveniles of common sole *Solea solea* in
235 the Seine estuarine nursery. The Seine Estuary is located on the North-West French coast, and opens up
236 in the English Channel (Figure 3). The Seine nursery covers a subtidal shallow area of 360 km²,
237 characterized by a mean depth of 8.2m, and muddy-fine sand sediments (Billen et al., 2001).



238

239 Figure 3: Map of the estuary of the Seine. The red dots represent the position of the stations were
 240 juveniles common soles were sampled.

241

2.4.2 Data

242 The common sole is a benthic-demersal flatfish of fishery interest, found in the muddy and
 243 shallow habitats of the Atlantic Ocean, as well as in the Black and Mediterranean seas. Within the
 244 nursery, juveniles mainly live in intertidal and subtidal mudflats, where they feed on benthic meiofauna
 245 and macrofauna (mainly copepods, shellfish and polychaetes) (Gibson et al., 2014; Morat, 2011).

246 Fish data were provided by the Cellule de Suivi du Littoral Normand (CLSN, research projects
 247 CAPES and Modhanour) from an historic beam-trawling survey conducted between 2000 and 2014 in
 248 the Seine estuary. Every month or two months, juvenile fish were sampled and measured in several
 249 stations in the estuary (Figure 3). The age-class to which the individuals belonged (*i.e.* G0 for the
 250 individuals born in the year, G1 for the ones born one year before the sampling or G2 for the ones born
 251 two years before the sampling) was also identified via Gaussian fitting on the size spectra, and provided
 252 by the Institut Français de Recherche pour l'Exploitation de la Mer (IFREMER). The birthdate was
 253 fixed on February 1st for all juveniles.

254 Satellite-based SST (sea surface temperature) observations were extracted from Pathfinder (1998-2009),
255 Ostia (2010), and Odyssea (2011-2014) products to construct 1998-2014 time series. The observations
256 were re-interpolated over a regular grid with 2.5*2.5 km cells and averaged over the outer Seine estuary
257 on a daily scale (See

258

259 Appendix B for further information on the temperature data).

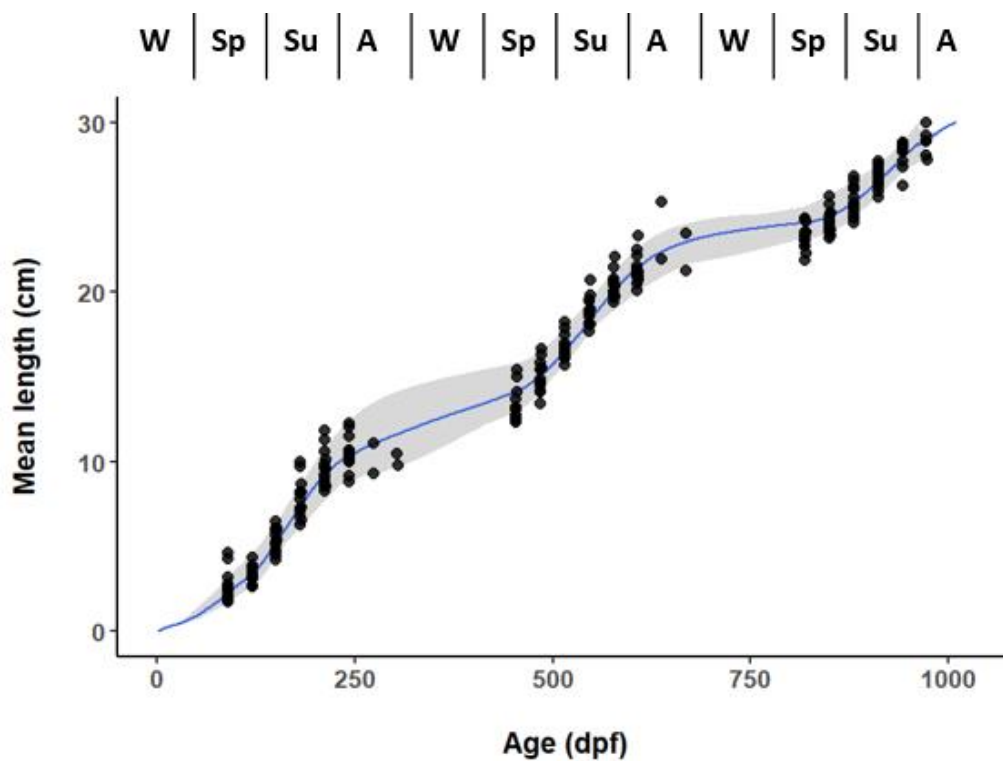
260 Concerning the implementation of the DEB model for the sole, we used the sets of DEB parameters
261 calibrated by Mounier et al. (2020) for males and females (see Appendix A).

262 **3. RESULTS**

263 **3.1 Energy intake over time**

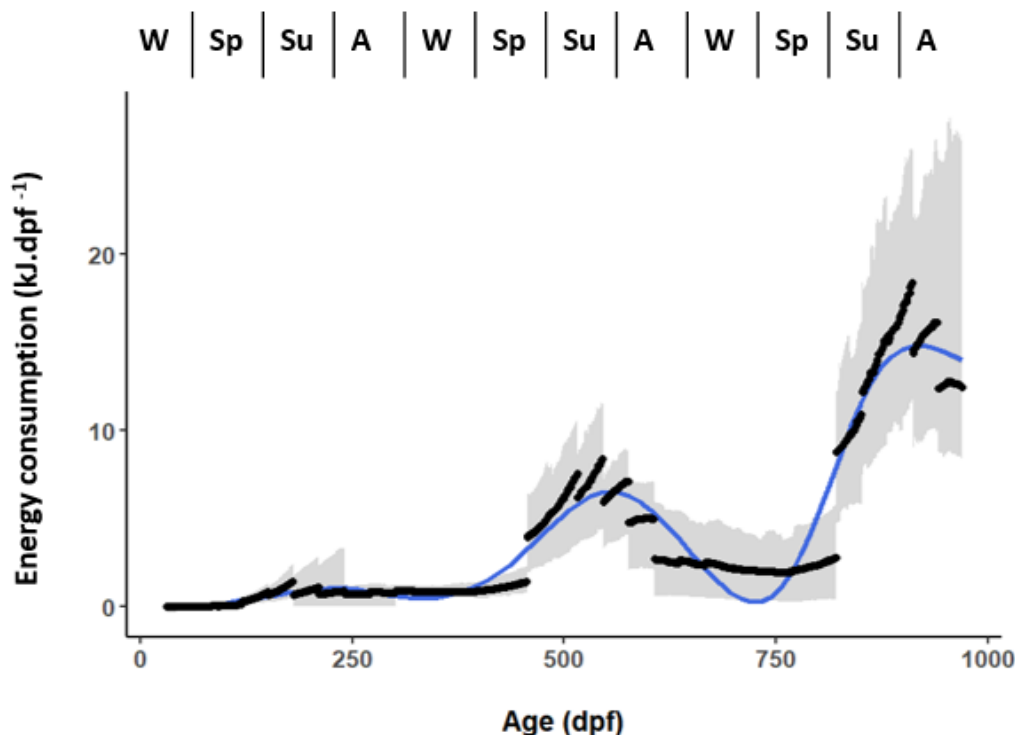
264 From the experienced temperatures, individual-specific food conditions were reconstructed to
265 adjust to observed growth data (Figure 4). The fit of the reconstructed growth trajectories with the
266 observed growth data for each cohort separately is shown in Appendix D. We simulated the daily energy
267 consumption of juveniles within the nursery (Figure 5). The daily energy consumption increases with
268 the age of the average individual. In addition, a seasonal pattern can be observed, with a high decrease
269 of energy consumption at the end of the growth season of the common soles (*i.e.*, late summer/autumn).
270 The breaks observed in the values of energy consumption are the consequence of keeping a relative food
271 condition constant between each observation (*i.e.* the average relative food condition for an entire time
272 period between two observations).

273



274

275 Figure 4: Observed mean lengths per dpf per cohort (black dots) over time (in days post fertilization),
 276 and estimations of lengths by the DEB model under experienced temperatures and individual-specific
 277 food conditions. The blue line represents the average estimated lengths, the grey area represents the
 278 range between the upper and lower values of estimated length. Capital letters correspond to the
 279 seasons (W = Winter, Sp = Spring, Su = Summer, A = Autumn).



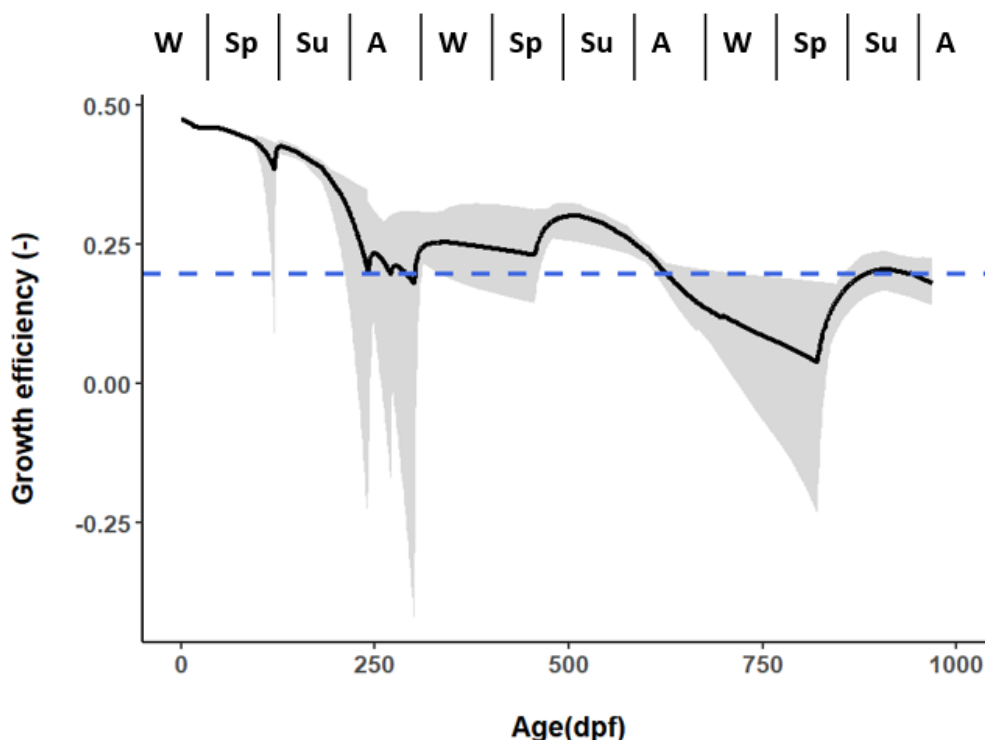
280

281 Figure 5: Energy consumption simulated by the DEB model over time (in days post fertilization) under
 282 experienced temperatures and individual-specific food conditions. The black dots represent the mean
 283 energy consumption for individuals of all cohorts. The blue line is a smoothed function of this energy
 284 consumption. The grey area represents the range between the upper and lower values of daily energy
 285 consumption. Capital letters correspond to the seasons (W = Winter, Sp = Spring, Su = Summer, A =
 286 Autumn).

287 3.2 Dynamic of growth efficiency

288 The growth efficiency coefficient estimated by the DEB shows a dynamic pattern dependent of
 289 the age and the seasons (Figure 6). The growth efficiency coefficient is overall decreasing over time
 290 with older individuals investing relatively less assimilated energy in growth compared to young
 291 individuals. In late spring, the coefficient increases while in autumn and winter it tends to decrease for
 292 all age-classes, with even negative growth coefficients observed for some cohorts. In opposition, the
 293 growth efficiency coefficient proposed by Day et al. (2021) for soles based on the model of EE (Tableau
 294 et al., 2019) is constant over season and age (blue line in Figure 6). During the first two years in the
 295 nursery (approximately between 90 and 730 dpf), the DEB model predicts a growth efficiency

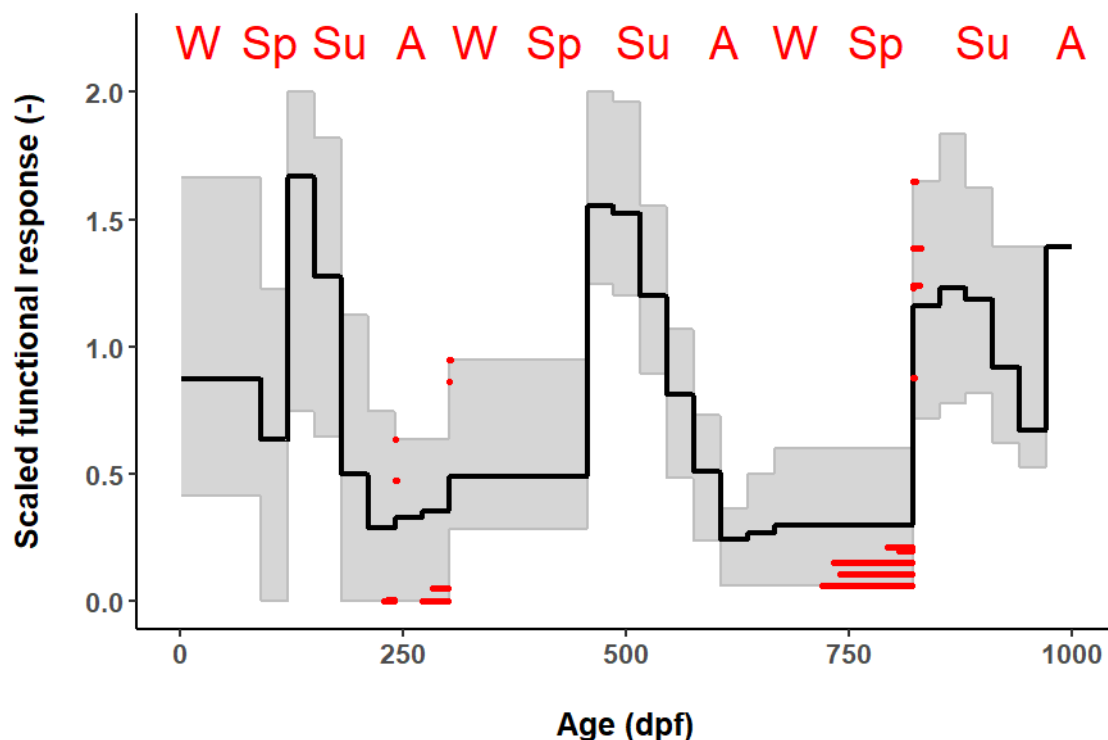
296 coefficient that is generally higher than the one considered in the model of EE, while the opposite is
 297 observed during the last year (between 730 and 970).



298
 299 Figure 6: Evolution of the growth efficiency coefficient for an average individual over time (in days post
 300 fertilization). Blue dashed line is the constant growth efficiency coefficient considered by the EE model
 301 of Tableau et al. (2019) for the *soleidae* (Day et al., 2021). Black solid line is the mean growth
 302 efficiency coefficient estimated by the DEB model. The grey area is the range between the lower and
 303 the upper values of the growth efficiency coefficient, for the cohorts between 2000 to 2014. Capital
 304 letters correspond to the seasons (W = Winter, Sp = Spring, Su = Summer, A = Autumn).

305 3.3 Link between growth efficiency and relative food availability

306 The mean scaled functional response (*i.e.* individual-specific food availability) shows also a
 307 seasonal trend, with highest values in summer and lowest in winter (even null values) (Figure 7).
 308 Regarding the link between growth efficiency and the scaled functional response, it appears that periods
 309 of shrinking (*i.e.* when the growth efficiency is negative) correspond to periods when the scaled
 310 functional response is null or very low, or days following this period (Figure 7).

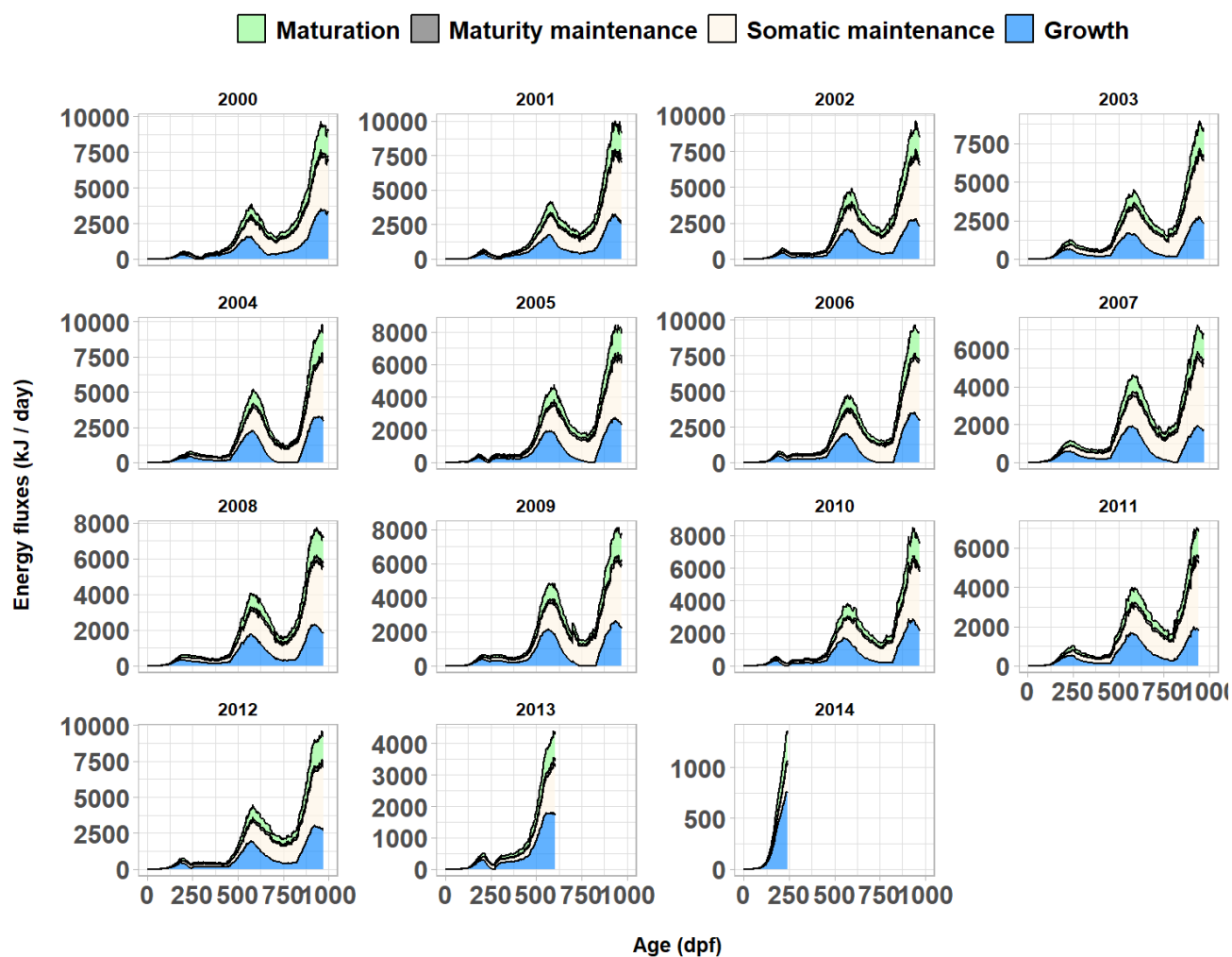


311
 312 Figure 7: Evolution of the scaled functional response (*i.e.*, individual-scaled food availability)
 313 over time (in days post fertilization). The black line corresponds to the average scaled
 314 functional response. The grey area corresponds to the range between the lower and upper
 315 values of the scaled functional response, for the cohorts between 2000 and 2014. The red
 316 dots correspond to values of scaled functional response for days when the growth efficiency
 317 (K) is negative. Capital letters correspond to the seasons (W = Winter, Sp = Spring, Su =
 318 Summer, A = Autumn).

319 3.4 Energy partitioning

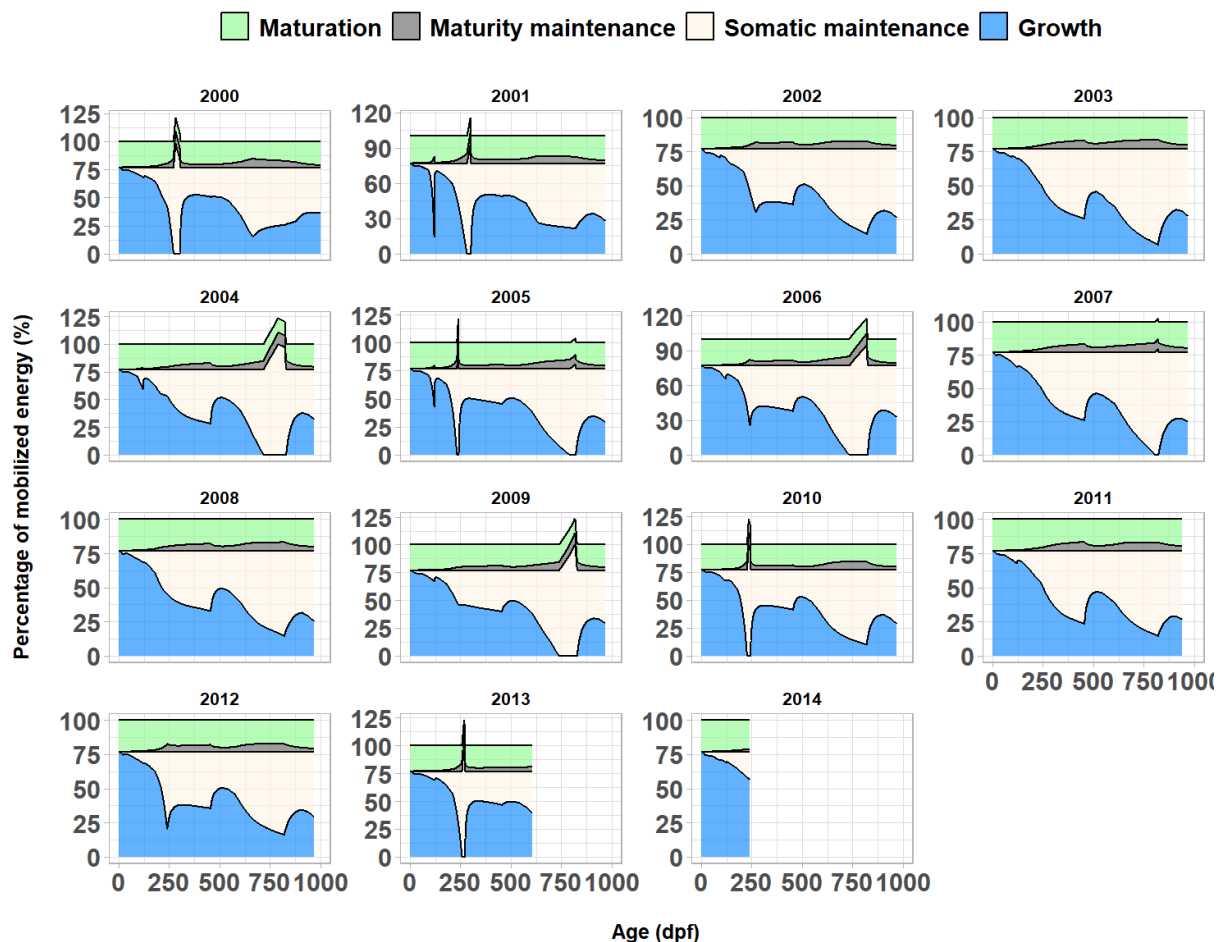
320 Our method allows studying energy partitioning between the main metabolic processes
 321 considered by the DEB model (*i.e.* growth, maturation and maintenance processes) through time,
 322 independently for each cohort. The study of the absolute fluxes (kJ/day) towards each metabolic process
 323 (Figure 8) clearly shows the temporal variability of the energetic fluxes, with very low total energy
 324 budget from late autumn to early spring. A decrease in the percentage of energy allocated to the growth
 325 during late summer/autumn (around 250 dpf and around 800 dpf) is also observed Figure 9, even with
 326 some moments with no energy allocated to growth (Figure 8, Figure 9). The decrease in energy
 327 allocation to growth is actually due to the increase in the proportion of maintenance processes to the

328 total energy budget, mainly the somatic maintenance (Figure 9). Also, during the end of
 329 summer/autumn, the cumulative percentage of the energy allocated to the main metabolic processes
 330 considered in the DEB model exceeds 100% suggesting a period of high nutritional stress for juveniles
 331 during some years.



332

333 Figure 8: Energy fluxes towards maturation, maintenance of maturity, somatic maintenance and growth
 334 for an average individual of cohorts 2000 to 2014. Information for the G2 born in 2013, as well as for the
 335 G1 and G2 born in 2014, is not given, as growth data were not provided after 2014.



336

337 Figure 9: Percentages of mobilized energy allocated to maturation, maintenance of maturity, somatic
 338 maintenance and growth for an average individual of cohorts 2000 to 2014. Information for the G2
 339 born in 2013, as well as for the G1 and G2 born in 2014, is not given, as growth data were not
 340 provided after 2014.

341

342 4. DISCUSSION

343 4.1 Highlights

344 This study applies a bioenergetic approach based on DEB theory to (i) investigate the potential
 345 of DEB model to highlight nutritional stresses for individuals and (ii) test the trophic limitation
 346 hypothesis for juvenile soles from a metabolic point of view. We reconstructed the scaled functional
 347 response, *i.e.*, the individual-specific food availability, from observed growth patterns and the daily
 348 temperature experienced by the individuals using inverse-DEB modelling. Although f corresponds to

349 the food actually ingested by the individual (it takes into account food density, but also competition), it
350 can be used as a proxy of food conditions available in the environment (Freitas et al., 2011). Classic
351 estimations of food availability require extensive samplings of the benthic ecosystem, identification of
352 potential prey and hypotheses on their energetic density. Provided that the model parameters are
353 available and reliable, our method is time- and cost-efficient while accounting for temperature changes
354 over time. This approach allows also describing in an accurate and dynamic way the energy assimilation
355 and energy partitioning for an individual over time, under the experienced environmental conditions,
356 but also in new environments such as those expected in the context of global warming. Finally, our
357 approach allows identifying periods of nutritional stress, consequence of trophic limitation. Altogether,
358 our method supports the hypothesis of trophic limitation during autumn in the Seine estuary, and can
359 help predict energetic needs in marine nurseries and associated ecological consequences.

360 **4.2 Food ingestion dynamics from observed growth trajectories**

361 The energy consumption of organisms is particularly difficult to assess, because it depends on
362 several physiological and environmental factors, as well as on the life stage of the individual (Kooijman,
363 2010; Yamashita *et al.*, 2001). The quantitative study of the individual-specific food availability allowed
364 at a daily scale by the inverse-DEB modelling may interestingly complement other feeding approaches
365 (stable isotopes and gut contents analyses) that can give insights of quantitative contributions of source
366 and prey but not at a fine temporal resolution. The back-calculation of food ingestion and assimilation
367 from growth patterns has already been used for the bay of Biscay Anchovies *Engraulis encrasicolus*
368 (Pecquerie et al., 2012), as well as to test trophic limitation hypothesis for the sand goby over the period
369 of nursery residence (Freitas et al., 2011). However, Pecquerie et al. (2012) did not use the temperatures
370 really experienced by the fish, reducing the precision of the calculation of the food ingestion. In addition,
371 the method used in Freitas et al. (2011) allowed to reconstruct the average individual-specific food
372 conditions over the entire lifespan based on maximum sizes of fish.

373 We have the capacity with our method to describe fluctuations in the individuals' energy
374 consumption. The decrease in energy consumption in late summer/autumn might be related to the

375 combined effects of (i) the still high temperatures and (ii) the decrease in individual-specific food
376 availability (see Figure 7). This first result showing the reconstructed food ingestion is important
377 because energy consumption of individuals is one of the main factors that allow understanding the
378 trophic limitation, and DEB model directly links energy consumption with individual-specific food
379 availability. Furthermore, the quantitative knowledge on feeding history is essential for the study of the
380 energy partitioning made in this study.

381 **4.3 Studying energy partitioning to understand the trophic limitation from a** 382 **metabolic point of view**

383 **4.3.1 Energy allocated to growth**

384 DEB theory deeply structures our knowledge on energy partitioning, particularly between
385 maintenance and growth during fish's entire life cycle including first life stages (Kooijman, 2010; van
386 der Meer, 2006). A DEB model considers that the individual consumes energy, even when it does not
387 grow, to maintain its organism and to mature. The increase with the age of energy requirement for
388 maintenance processes is the consequence of a maintenance proportional to the volume V and maturity
389 of the organism while assimilated energy is proportional to $V^{2/3}$ (see Table 1). This leads to a decrease
390 over time of the growth efficiency coefficient. This coefficient is also affected by seasonal cycle, with
391 a decrease of relative energy allocated towards growth in late summer/autumn. This decrease coincides
392 with an increase in the proportion of somatic maintenance processes to the total energy budget (Figure
393 9). However, more work is needed in order to investigate whether this increase of proportion of energy
394 allocated to the somatic maintenance is due to (i) an increase in the absolute maintenance requirements,
395 possibly linked to environmental conditions, or (ii) to the observed decrease in the energy assimilation
396 (figure 5). In the latter case, the observed seasonal decrease in energy allocated towards growth could
397 be an index of trophic limitation. Indeed, if the individual cannot assimilate enough energy, it allocates
398 in priority energy to maintenances, rather than growth, and this phenomenon is taken into account in
399 DEB theory (Kooijman, 2010).

400 **4.3.2 Nutritional stress**

401 The study of energy partitioning over time shows that for multiple years, the amount of energy
402 theoretically allocated to the metabolic compartment exceeds periodically the energy the fish can
403 mobilize from its environment (Figure 9). This result indicates a potential nutritional stress: the average
404 individual is not able to mobilize sufficient energy from its food to balance energetic needs for
405 maintenance. In this case, DEB theory allows to mobilize energy from the individual's structure
406 (Kooijman, 2001). This is possible via processes of shrinking, observed when k (*i.e.* growth efficiency
407 coefficient) is negative. Our results show that these periods of shrinking correspond to periods when the
408 f value (*i.e.* individual-specific food availability) is very low (Figure 7). During a few days just after a
409 period of low individual-specific food availability, k can remain negative, even if the mean value of f
410 has risen. We interpret this by a little delay time after a nutritional stress, before the individual can re-
411 allocate energy into growth.

412 These periods of nutritional stress can reflect critical trophic limitation periods, in late
413 summer/autumn. This is coherent with the results of previous studies on the Seine estuarine nursery that
414 identify this phenomenon at the same period of the year (Day et al., 2021; Saulnier et al., 2020).

415 **4.4 Limits and perspectives**

416 Some authors discuss the use of growth data for estimation of trophic limitation of nursery (Le
417 Pape & Bonhommeau, 2015). Indeed, this implies the risk to overestimate the growth, hence energy
418 consumption of individuals because of (i) apparent growth rates of only survival fish, and in this case
419 study (ii) selectivity of the beam trawl or (ii) omitted immigration and emigration processes (bigger fish
420 might migrate to deeper areas). However, if indices of trophic limitation are visible regarding larger
421 individuals, we can assume that this will be even more the case for small individuals. Another limit of
422 our method could be the fitting of the lengths estimated by the DEB model with length-at-age data
423 obtained with a fixed birthdate. It would be interesting to investigate the effect of the birthdate on the
424 results. Indeed, the spawning period, and thus the timing of colonization of estuaries by young stages
425 are variable among sub-populations, depending on environmental conditions (Amara et al., 2000).

426 Moreover, our approach considers two major environmental factors (*i.e.*, temperature and food
427 availability) on the individual's metabolism. However, other environmental factors affected by global
428 change may influence species' energetic needs. For example, oxygen availability (Gibson, 1994), or
429 pollution (Mounier et al., 2020) constitute stressors that might modify fish's metabolism, including
430 energy assimilation (Sadoul & Vijayan, 2016). This is particularly true in coastal nurseries, where
431 organisms are subjected to important environmental gradients, and rapid human-induced changes
432 (McLusky & Elliott, 2004).

433 We assumed here that the f reconstructed using the method presented in this paper can be used
434 to explore the potential trophic limitation of nursery grounds as it is, to some extent, representative of
435 the average overall food conditions in the nursery. This is all the more relevant that preliminary results
436 in this direction show for instance that there is a significant and positive link between the mean annual
437 values of the scaled functional response (all individuals considered) and the mean annual values of the
438 scaled functional response for each age class G0, G1 and G2 (see Appendix E). However, although we
439 didn't highlight differences between age-classes (that could be interpreted in terms of competition for
440 instance), a more in-depth year-to-year comparison of results of individual-specific energy availability
441 and energy partitioning by age class, combined with data of environmental conditions (*i.e.* temperature,
442 juveniles' abundance leading to competition, and prey production) will substantially improve our
443 understanding of trophic limitation.

444 We carried out this study on an average individual of each cohort, as the aim was to investigate
445 the potential of DEB models to reconstruct energy ingestion and highlight nutritional stresses for
446 individuals. However, the use of this method to simulate several individuals will be particularly
447 interesting, allowing to (i) consider inter-individual variations e.g. in $\{p_{Am}\}$, and (ii) to extrapolate our
448 results at the population scale, e.g. by including a probability to die when a nutritional stress occurs,
449 which was not done here.

450 It would also be interesting to generalize the method to other study sites and to explore how
451 other species belonging to the juvenile fish community can be considered together.

452 To conclude, our method based on the study of energy intake and energy partitioning at an
453 individual scale responds to some difficulties raised in the concrete identification of signs of a trophic
454 limitation for organisms (Ciotti et al., 2014; Le Pape & Bonhommeau, 2015). We showed that it is
455 possible with our method to assess individual's food intake from their observed lengths, and results of
456 energy partitioning put forward indices of trophic limitation such as growth reduction and periods of
457 nutritional stress. Being able to identify periods of non-growing and nutritional stress is also interesting
458 in the context of species' conservation, and fisheries management, as it extends our knowledge on
459 underlying processes that affect fish populations' renewal, hence dynamic. All this will give a better
460 insight of the nurseries' functioning and its evolution.

ACKNOWLEDGMENT

We want to thank Florence Mounier for providing the species specific parameters of the DEB model and for early discussions during the process. We also thank the Seine Normandy water agency and HAROPA PORT | Le Havre who financed the data collection, Sylvain Duhamel at the CSLN (Cellule du Suivi du Littoral Normand) for collecting the fish data, and the GIP Seine Aval for funding the Modhanour project who cleaned and provided the data. And, finally, we really want to acknowledge the two anonymous reviewers of the initial draft of this paper. They significantly helped us to improve the manuscript.

FUNDINGS

This research did not receive any specific grant from funding agencies in the public, commercial, or not-for-profit sectors.

CONFLICT OF INTEREST

The authors declare no conflict of interest.

AUTHORS' CONTRIBUTIONS

Marion Lefebvre du Prey: Methodology, Software, Formal analysis, writing – Original draft, Visualization. Jérémy Lobry: Conceptualization, Methodology, Validation, Writing – Original draft. Anik Brind'Amour: Investigation, Data Curation, Writing- Review and Editing. Hervé Le Bris: Investigation, Data curation, Writing – Review and Editing, Supervision. Bastien Sadoul: Conceptualization, Methodology, Validation, Writing – Original draft, Supervision.

DATA AVAILABILITY STATEMENT

The data used for this work will be available upon acceptance of the manuscript on the database data.inrae.fr.

REFERENCES

- Amara, R., Laffargue, P., Dewarumez, J. M., Maryniak, C., Lagardère, F., & Luzac, C. (2001). Feeding ecology and growth of 0-group flatfish (sole, dab and plaice) on a nursery ground (Southern Bight of the North Sea). *Journal of Fish Biology*, *58*(3), 788–803.
- Amara, R., Lagardere, F., Desaunay, Y., & Marchand, J. (2000). Metamorphosis and estuarine colonisation in the common sole, *Solea solea* (L.): Implications for recruitment regulation. *Oceanologica Acta*, *23*(4), 469–484.
- Augustine, S., Litvak, M. K., & Kooijman, S. A. L. M. (2011). Stochastic feeding of fish larvae and their metabolic handling of starvation. *Journal of Sea Research*, *66*(4), 411–418.
<https://doi.org/10.1016/j.seares.2011.07.006>
- Billen, G., Garnier, J., Ficht, A., & Cun, C. (2001). Modeling the response of water quality in the Seine River estuary to human activity in its watershed over the last 50 years. *Estuaries*, *24*(6), 977–993. <https://doi.org/10.2307/1353011>
- Byrd, R. H., Lu, P., Nocedal, J., & Zhu, C. (1995). A limited memory algorithm for bound constrained optimization. *SIAM Journal on Scientific Computing*, *16*(5), 1190–1208.
- Cardoso, J. F. M. F., Freitas, V., de Paoli, H., Witte, J. IJ., & van der Veer, H. W. (2016). Growth conditions of 0-group plaice *Pleuronectes platessa* in the western Wadden Sea as revealed by otolith microstructure analysis. *Journal of Sea Research*, *111*, 88–96.
<https://doi.org/10.1016/j.seares.2016.01.010>
- Cardoso, J. F. M. F., Witte, J. IJ., & van der Veer, H. W. (2006). Intra- and interspecies comparison of energy flow in bivalve species in Dutch coastal waters by means of the Dynamic Energy Budget (DEB) theory. *Journal of Sea Research*, *56*(2), 182–197.
<https://doi.org/10.1016/j.seares.2006.03.011>

- Ciotti, B. J., Targett, T. E., Nash, R. D., & Geffen, A. J. (2014). Growth dynamics of European plaice *Pleuronectes platessa* L. in nursery areas: A review. *Journal of Sea Research*, 90, 64–82.
- Collie, J. (1987). Food consumption by yellowtail flounder in relation to production of its benthic prey. *Marine Ecology Progress Series*, 36, 205–213. <https://doi.org/10.3354/meps036205>
- Daewel, U., Peck, M. A., & Schrum, C. (2011). Life history strategy and impacts of environmental variability on early life stages of two marine fishes in the North Sea: An individual-based modelling approach. *Canadian Journal of Fisheries and Aquatic Sciences*, 68(3), 426–443. <https://doi.org/10.1139/F10-164>
- Day, L., Brind'Amour, A., Cresson, P., Chouquet, B., & Le Bris, H. (2021). Contribution of estuarine and coastal habitats within nursery to the diets of juvenile fish in spring and autumn. *Estuaries and Coasts*, 44(4), 1100–1117.
- Freitas, V., Cardoso, J. F., Santos, S., Campos, J., Drent, J., Saraiva, S., Witte, J. I., Kooijman, S. A., & Van der Veer, H. W. (2009). Reconstruction of food conditions for Northeast Atlantic bivalve species based on Dynamic Energy Budgets. *Journal of Sea Research*, 62(2–3), 75–82.
- Freitas, V., Kooijman, S., & van der Veer, H. (2012). Latitudinal trends in habitat quality of shallow-water flatfish nurseries. *Marine Ecology Progress Series*, 471, 203–214. <https://doi.org/10.3354/meps10025>
- Freitas, V., Lika, K., Witte, J. I., & der Veer, H. W. van. (2011). Food conditions of the sand goby *Pomatoschistus minutus* in shallow waters: An analysis in the context of Dynamic Energy Budget theory. *Journal of Sea Research*, 66(4), 440–446. <https://doi.org/10.1016/j.seares.2011.05.008>
- Gibson, R. N., Nash, R. D., Geffen, A. J., & Van der Veer, H. W. (2014). *Flatfishes: Biology and exploitation*. John Wiley & Sons.
- Gilliers, C., Le Pape, O., Désaunay, Y., Morin, J., Guéroult, D., & Amara, R. (2006). Are growth and density quantitative indicators of essential fish habitat quality? An application to the common sole *Solea solea* nursery grounds. *Estuarine, Coastal and Shelf Science*, 69(1), 96–106. <https://doi.org/10.1016/j.ecss.2006.02.006>

- Kooijman, B. (2010). *Dynamic energy budget theory for metabolic organisation*. Cambridge university press.
- Kooijman, S. a. l. m. (2001). Quantitative aspects of metabolic organization: A discussion of concepts. *Philosophical Transactions of the Royal Society of London. Series B: Biological Sciences*, 356(1407), 331–349. <https://doi.org/10.1098/rstb.2000.0771>
- Lavaud, R., Rannou, E., Flye-Sainte-Marie, J., & Jean, F. (2019). Reconstructing physiological history from growth, a method to invert DEB models. *Journal of Sea Research*, 143, 183–192.
- Le Pape, O., & Bonhommeau, S. (2015). The food limitation hypothesis for juvenile marine fish. *Fish and Fisheries*, 16(3), 373–398. <https://doi.org/10.1111/faf.12063>
- Le Pape, O., Holley, J., Guérault, D., & Désaunay, Y. (2003). Quality of coastal and estuarine essential fish habitats: Estimations based on the size of juvenile common sole (*Solea solea* L.). *Estuarine, Coastal and Shelf Science*, 58(4), 793–803. [https://doi.org/10.1016/S0272-7714\(03\)00185-9](https://doi.org/10.1016/S0272-7714(03)00185-9)
- McLusky, D. S., & Elliott, M. (2004). *The Estuarine Ecosystem: Ecology, Threats and Management*. OUP Oxford.
- Meyer, S., Caldarone, E. M., Chícharo, M. A., Clemmesen, C., Faria, A. M., Faulk, C., Folkvord, A., Holt, G. J., Høie, H., Kanstinger, P., Malzahn, A., Moran, D., Petereit, C., Støttrup, J. G., & Peck, M. A. (2012). On the edge of death: Rates of decline and lower thresholds of biochemical condition in food-deprived fish larvae and juveniles. *Journal of Marine Systems*, 93, 11–24. <https://doi.org/10.1016/j.jmarsys.2011.09.010>
- Morat, F. (2011). *Influence des apports rhodaniens sur les traits d'histoires de vie de la sole commune (Solea Solea): Apports de l'analyse structurale et minéralogique des otolithes*. [These de doctorat, Aix-Marseille 2]. <https://www.theses.fr/2011AIX22126>
- Mounier, F. (2019). *Modelling mechanistic bioaccumulation of organic contaminants (PCBs and PFASs) in fish in the context of global change: Application to the Gironde estuary juvenile common sole* [Phdthesis, Université de Bordeaux]. <https://theses.hal.science/tel-03183574>
- Mounier, F., Loizeau, V., Pecquerie, L., Drouineau, H., Labadie, P., Budzinski, H., & Lobry, J. (2020). Dietary bioaccumulation of persistent organic pollutants in the common sole *Solea*

- solea in the context of global change. Part 2: Sensitivity of juvenile growth and contamination to toxicokinetic parameters uncertainty and environmental conditions variability in estuaries. *Ecological Modelling*, 431, 109196. <https://doi.org/10.1016/j.ecolmodel.2020.109196>
- Nash, R., Geffen, A., Burrows, M., & Gibson, R. (2007). Dynamics of shallow-water juvenile flatfish nursery grounds: Application of the self-thinning rule. *Marine Ecology Progress Series*, 344, 231–244. <https://doi.org/10.3354/meps06933>
- Neill, W. H., Miller, J. M., Van Der Veer, H. W., & Winemiller, K. O. (1994). Ecophysiology of marine fish recruitment: A conceptual framework for understanding interannual variability. *Netherlands Journal of Sea Research*, 32(2), 135–152. [https://doi.org/10.1016/0077-7579\(94\)90037-X](https://doi.org/10.1016/0077-7579(94)90037-X)
- Nicolas, D., Le Loc'h, F., Désaunay, Y., Hamon, D., Blanchet, A., & Le Pape, O. (2007). Relationships between benthic macrofauna and habitat suitability for juvenile common sole (*Solea solea*, L.) in the Vilaine estuary (Bay of Biscay, France) nursery ground. *Estuarine, Coastal and Shelf Science*, 73(3–4), 639–650. <https://doi.org/10.1016/j.ecss.2007.03.006>
- Nunn, A. D., Tewson, L. H., & Cowx, I. G. (2012). The foraging ecology of larval and juvenile fishes. *Reviews in Fish Biology and Fisheries*, 22(2), 377–408. <https://doi.org/10.1007/s11160-011-9240-8>
- Pecquerie, L., Fablet, R., de Pontual, H., Bonhommeau, S., Alunno-Bruscia, M., Petitgas, P., & Kooijman, S. (2012). Reconstructing individual food and growth histories from biogenic carbonates. *Marine Ecology Progress Series*, 447, 151–164. <https://doi.org/10.3354/meps09492>
- Poiesz, S. S. H., van Leeuwen, A., Soetaert, K., Witte, J. IJ., Zaat, D. S. C., & van der Veer, H. W. (2020). Is summer growth reduction related to feeding guild? A test for a benthic juvenile flatfish sole (*Solea solea*) in a temperate coastal area, the western Wadden Sea. *Estuarine, Coastal and Shelf Science*, 235, 106570. <https://doi.org/10.1016/j.ecss.2019.106570>
- Rochette, S., Rivot, E., Morin, J., Mackinson, S., Riou, P., & Le Pape, O. (2010). Effect of nursery habitat degradation on flatfish population: Application to *Solea solea* in the Eastern Channel

- (Western Europe). *Journal of Sea Research*, 64(1–2), 34–44.
<https://doi.org/10.1016/j.seares.2009.08.003>
- Sadoul, B., & Vijayan, M. M. (2016). Stress and Growth. In *Fish Physiology* (Vol. 35, pp. 167–205). Elsevier. <https://doi.org/10.1016/B978-0-12-802728-8.00005-9>
- Saulnier, E., Le Bris, H., Tableau, A., Dauvin, J. C., & Brind'Amour, A. (2020). Food limitation of juvenile marine fish in a coastal and estuarine nursery. *Estuarine, Coastal and Shelf Science*, 241, 106670. <https://doi.org/10.1016/j.ecss.2020.106670>
- Seitz, R. D., Wennhage, H., Bergström, U., Lipcius, R. N., & Ysebaert, T. (2014). Ecological value of coastal habitats for commercially and ecologically important species. *ICES Journal of Marine Science*, 71(3), 648–665. <https://doi.org/10.1093/icesjms/fst152>
- Selleslagh, J., & Amara, R. (2013). Effect of starvation on condition and growth of juvenile plaice *Pleuronectes platessa*: Nursery habitat quality assessment during the settlement period. *Journal of the Marine Biological Association of the United Kingdom*, 93(2), 479–488. <https://doi.org/10.1017/S0025315412000483>
- Tableau, A., Brind'Amour, A., Woillez, M., & Le Bris, H. (2016). Influence of food availability on the spatial distribution of juvenile fish within soft sediment nursery habitats. *Journal of Sea Research*, 111, 76–87. <https://doi.org/10.1016/j.seares.2015.12.004>
- Tableau, A., Le Bris, H., Saulnier, E., Le Pape, O., & Brind'Amour, A. (2019). Novel approach for testing the food limitation hypothesis in estuarine and coastal fish nurseries. *Marine Ecology Progress Series*, 629, 117–131. <https://doi.org/10.3354/meps13090>
- van der Meer, J. (2006). An introduction to Dynamic Energy Budget (DEB) models with special emphasis on parameter estimation. *Journal of Sea Research*, 56(2), 85–102. <https://doi.org/10.1016/j.seares.2006.03.001>
- van der Veer, H., Freitas, V., Koot, J., Witte, J., & Zuur, A. (2010). Food limitation in epibenthic species in temperate intertidal systems in summer: Analysis of 0-group plaice *Pleuronectes platessa*. *Marine Ecology Progress Series*, 416, 215–227. <https://doi.org/10.3354/meps08786>

van der Veer, H., Tulp, I., Witte, J., Poiesz, S., & Bolle, L. (2022). Changes in functioning of the largest coastal North Sea flatfish nursery, the Wadden Sea, over the past half century. *Marine Ecology Progress Series*, 693, 183–201. <https://doi.org/10.3354/meps14082>

Van Der Veer, H. W., Berghahn, R., & Rijnsdorp, A. D. (1994). Impact of juvenile growth on recruitment in flatfish. *Netherlands Journal of Sea Research*, 32(2), 153–173. [https://doi.org/10.1016/0077-7579\(94\)90038-8](https://doi.org/10.1016/0077-7579(94)90038-8)

Vinagre, C., & Cabral, H. N. (2008). Prey consumption by the juvenile soles, *Solea solea* and *Solea senegalensis*, in the Tagus estuary, Portugal. *Estuarine, Coastal and Shelf Science*, 78(1), 45–50. <https://doi.org/10.1016/j.ecss.2007.11.009>

APPENDICES

Appendix A: Dynamic Energy Budget model

Parameters of the DEB model for *Solea solea*:

Table A.1: table of parameters of the DEB model for a juvenile of the common sole, *Solea solea*, with their description, unit, and values. All the parameters used in this study were found in Mounier et al. (Mounier et al., 2020). All rate parameters are expressed at the reference temperature $T_{ref} = 20^{\circ}\text{C} = 293\text{K}$.

Parameter	Description	Unit	Value	
			Females	Males
$\{\dot{p}_{Am}\}$	Maximum assimilation rate	$J.cm^{-2}.d^{-1}$	710	671
\dot{v}	Energy conductance	$cm.d^{-1}$	0.0724	
κ	Fraction of energy allocated to growth and somatic maintenance	-	0.7682	
$[\dot{p}_M]$	Somatic maintenance rate	$J.cm^{-3}.d^{-1}$	39.18	
$[E_G]$	Cost of structure	$J.cm^{-3}$	5430	
\dot{k}_j	Maturity maintenance rate coefficient	d^{-1}	0.002	
E_H^b	Maturation threshold at birth	J	0.285	
E_H^j	Maturation threshold at metamorphosis	J	6.039	
δ	Shape coefficient	-	0.171	

κ_X	Digestibility coefficient	-	0.8
κ_G	Growth efficiency	-	0.7705
T_L	Lower boundary of tolerance range	K	276
T_H	Upper boundary of tolerance range	K	303
T_A	Arrhenius temperature	K	5119
T_{AL}	Rate of decrease at lower boundary	K	50000
T_{AH}	Rate of decrease at upper boundary	K	100000
d_v	Density of structure	$g_d \cdot cm^{-3}$	0.2
q_v	Energy density of structure	$J \cdot g_d^{-1}$	20920

Temperature correction factor:

In DEB theory, all metabolic rates are scaled to body temperature evolution thanks to the correction of primary parameters with a temperature correction factor TC. The parameters $\{\dot{P}_{Am}\}$, \dot{v} , $[\dot{P}_M]$ and \dot{k}_j are therefore multiplied by TC. TC is calculated as:

$$TC = \exp\left(\frac{T_A}{T_{ref}} - \frac{T_A}{T}\right) \times \frac{1 + \exp\left(\frac{T_{AL}}{T_{ref}} - \frac{T_{AL}}{T_L}\right) + \exp\left(\frac{T_{AH}}{T_H} - \frac{T_{AH}}{T_{ref}}\right)}{1 + \exp\left(\frac{T_{AL}}{T} - \frac{T_{AL}}{T_L}\right) + \exp\left(\frac{T_{AH}}{T_H} - \frac{T_{AH}}{T}\right)}$$

Appendix B: Data of temperature

The temperatures used for this study are sea surface temperatures (SST) from satellite observations, because bottom temperature data were not available in the Seine Estuary throughout each sampled year (see figure B.1.a). To ensure the reliability of the use of SST, we compared SST and bottom temperatures for the dates when both data were available. SST and bottom temperatures are significantly correlated, with a Pearson's coefficient of 0.96 (see Figure B.1.b).

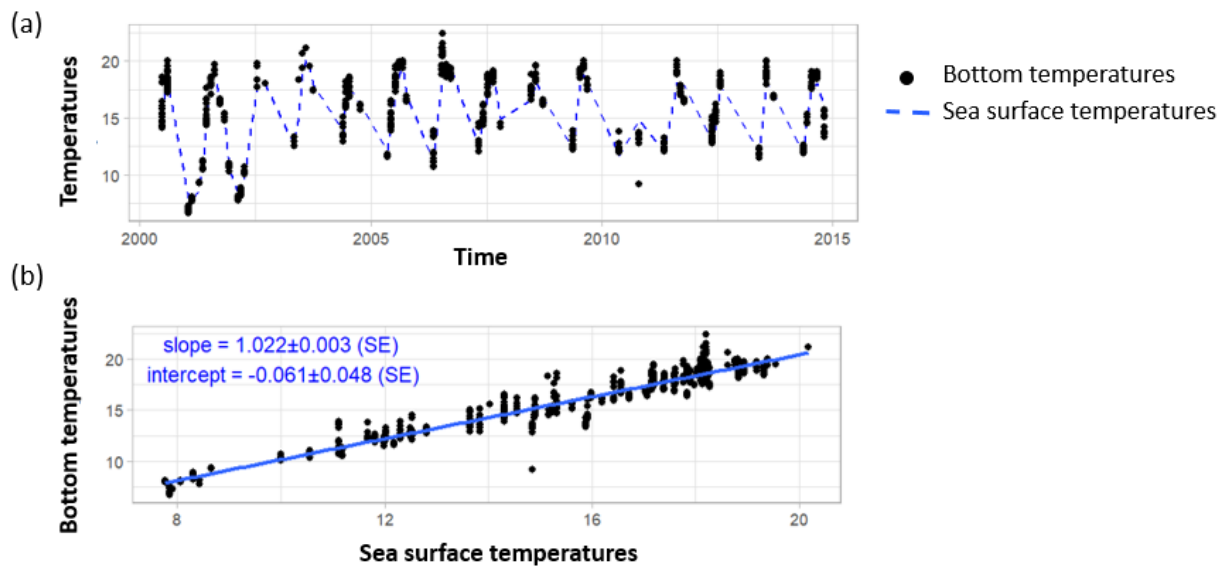


Figure B.1: (a) Temperatures available for the Seine estuary from 1998 to 2014. The black dots represent the bottom temperatures; the blue dashed line represents the sea surface temperatures. (b) Correlation of the sea surface temperatures and the bottom temperatures for the dates between 1998 and 2014 when they are both available in the Seine estuary.

Appendix C: Distribution of the scaled functional response

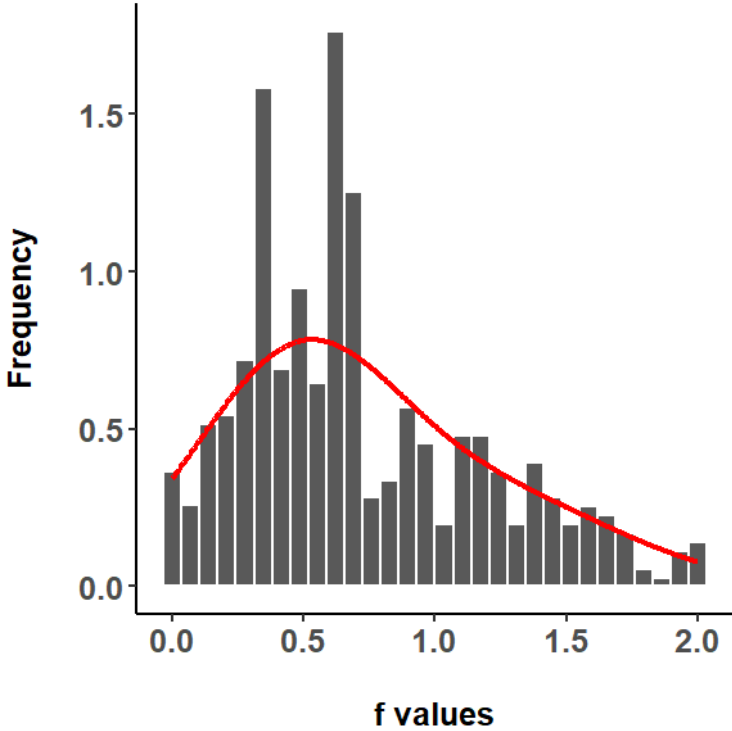


Figure C.1: Histogram and distribution (red line) of values of f that are back-calculated in the inverse-DEB modelling from the observed lengths of juvenile fish.

Appendix D: Fit of the growth trajectories reconstructed by the DEB model under experienced environmental conditions with the observed mean lengths data, for each cohort

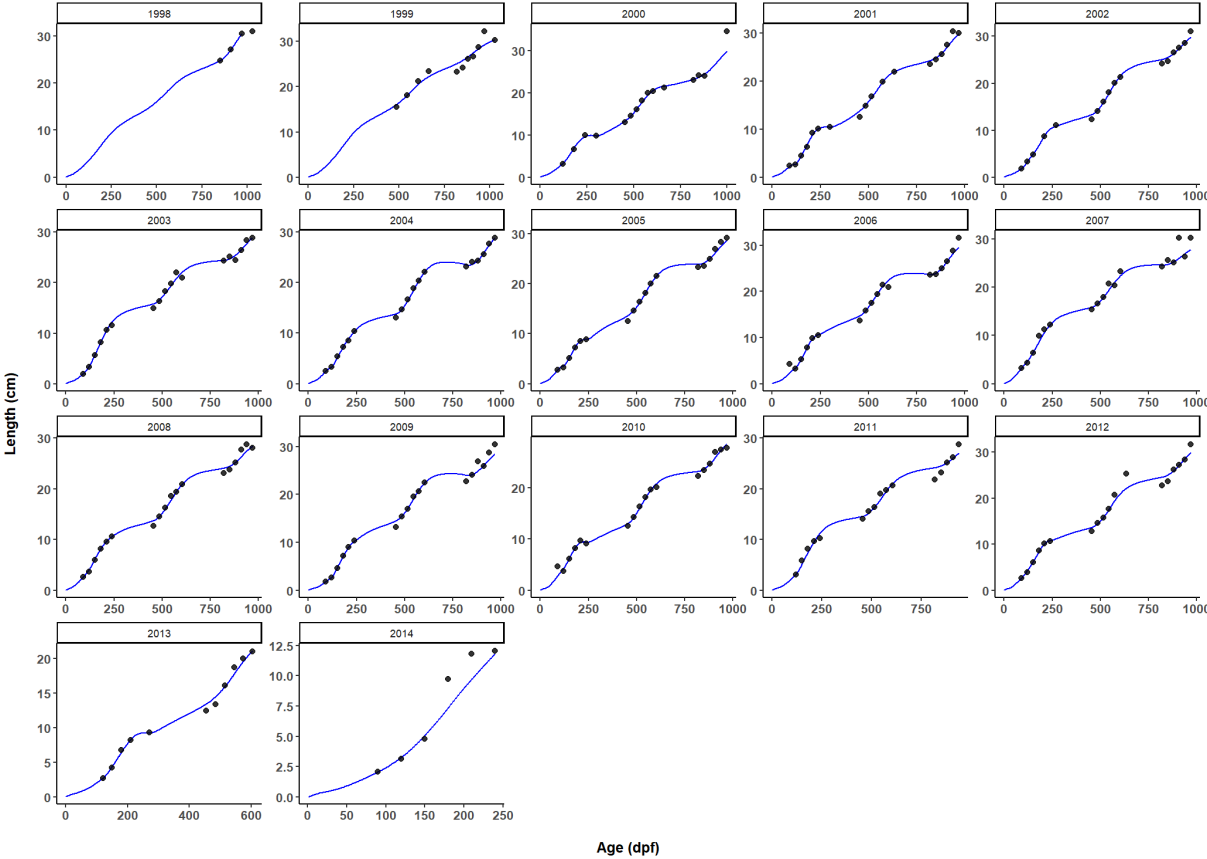


Figure D.1: Observed mean lengths (black dots) over time (in days post fertilization), and estimations of lengths by the DEB model under experienced temperatures and relative food conditions, for each cohort. The blue line represents the average estimated lengths over time for each cohort.

Appendix E: Comparison of mean annual values of the scaled functional response for all individuals and for each age-class.

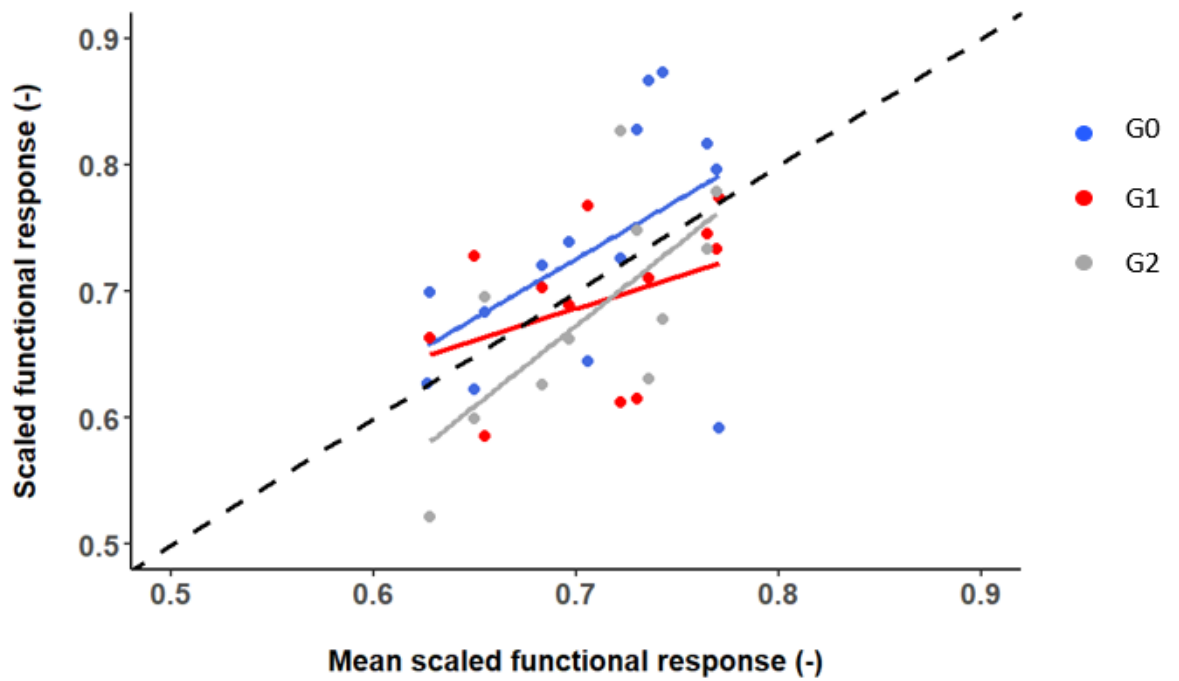


Figure E.1: Mean annual values of the scaled functional response (f) for each age-class (G0, G1 and G2) as a function of the mean annual values of the scaled functional response when considering all the individuals present in the nursery. Each point represents a year. The dashed line is the $x=y$ bisector.